



HAL
open science

Electrocoagulation process applied on pollutants treatment- experimental optimization and fundamental investigation of the crystal violet dye removal

Maryam Khadim Mbacké, Cheikhou Kane, Ndeye Oury Diallo, Codou Mar Diop, Fabien Chauvet, Maurice Comtat, Théodore Tzedakis

► To cite this version:

Maryam Khadim Mbacké, Cheikhou Kane, Ndeye Oury Diallo, Codou Mar Diop, Fabien Chauvet, et al.. Electrocoagulation process applied on pollutants treatment- experimental optimization and fundamental investigation of the crystal violet dye removal. *Journal of Environmental Chemical Engineering*, 2016, 4 (4), pp.4001-4011. 10.1016/j.jece.2016.09.002 . hal-01922251

HAL Id: hal-01922251

<https://hal.science/hal-01922251>

Submitted on 14 Nov 2018

HAL is a multi-disciplinary open access archive for the deposit and dissemination of scientific research documents, whether they are published or not. The documents may come from teaching and research institutions in France or abroad, or from public or private research centers.

L'archive ouverte pluridisciplinaire **HAL**, est destinée au dépôt et à la diffusion de documents scientifiques de niveau recherche, publiés ou non, émanant des établissements d'enseignement et de recherche français ou étrangers, des laboratoires publics ou privés.






OATAO is an open access repository that collects the work of Toulouse researchers and makes it freely available over the web where possible

This is an author's version published in: <http://oatao.univ-toulouse.fr/20493>

Official URL : <https://doi.org/10.1016/j.jece.2016.09.002>

To cite this version:

Mbacké, Maryam Khadim and Kane, Cheikhou and Diallo, Ndeye Oury and Diop, Codou Mar and Chauvet, Fabien  and Comtat, Maurice  and Tzedakis, Théo  *Electrocoagulation process applied on pollutants treatment- experimental optimization and fundamental investigation of the crystal violet dye removal.* (2016) *Journal of Environmental Chemical Engineering*, 4 (4). 4001-4011. ISSN 2213-3437

Any correspondence concerning this service should be sent to the repository administrator: tech-oatao@listes-diff.inp-toulouse.fr

Electrocoagulation process applied on pollutants treatment- experimental optimization and fundamental investigation of the crystal violet dye removal

Maryam Khadim Mbacké^a, Cheikhou Kane^a, Ndeye Oury Diallo^a, Codou Mar Diop^a, Fabien Chauvet^b, Maurice Comtat^b, Theo Tzedakis^{b,*,1}

^aLaboratoire d'Electrochimie et des Procédés Membranaires, Ecole Supérieure Polytechnique, Université Cheikh Anta Diop, B.P. 5085, Dakar Fann, Senegal

^bLaboratoire de Génie Chimique, UMR CNRS 5503, UFT-UTIII-PS, 118, route de Narbonne, Toulouse, France

ABSTRACT

The removal crystal violet (CV) from wastewater solutions was performed by electrocoagulation process based on an aluminum sacrificial anode. The effect of the operating parameters was experimentally investigated; a complete removal was achieved after 1 h electrolyses, and various 'short times' electrolyses were carried out to fundamentally investigate the main physical phenomena conditioning the flocs formation and allowing to achieve satisfactory coagulation rates.

A simplified theoretical model was proposed to predict the dye removal rate and to design an electrochemical reactor. It is based on a mechanism, involving $\text{Al}(\text{OH})_3$ oligomers formation, and competition between electrochemical oxidation and coagulation rate. The good agreement between simulation and experiments, allows i) the required kinetic constant value to be determined and ii) the limiting step to be defined as a reaction involving one $\text{Al}(\text{OH})_3$ fixing 4 molecules of the crystal violet. The presented results may be easily extrapolated to other dyes removal.

1. Introduction

Nowadays, environmental pollution due to industrial effluents constitutes a major problem. Over 10,000 synthetic dyes are extensively used in a large variety of industries, with an annual worldwide production higher than 7×10^8 kg; among them 5–10% is rejected as industrial effluents [1]. The dyes are widely used in textile industry, pulp and paper manufacturing, plastics, printing and microbiology [2,3]. To remove the synthetics dyes and their derivatives from wastewater, various techniques exist such as chemical coagulation, precipitation, electroflotation, adsorption on activated carbon, ion exchange through a liquid–liquid membrane, entrapment of the pollutant through a biological membrane and ultrafiltration. Furthermore, different advanced oxidation process, solar photocatalytic, UV and ozone treatments [4,5] have been also tested for the removal of such dyes from industrial wastewater. All

the above processes have been found to exhibit certain limitations: adsorption and coagulation are time consuming methods, biological methods suffer by the toxicity of dyestuffs [6], UV and other advanced oxidation processes require chemicals which introduce a secondary pollution [7]. In membrane separation technique, such as nanofiltration or reverse osmosis, "flux decline" is a common problem [8]. These technologies are usually uneconomical for high flow rate treatments and namely for wastes containing low contaminant concentrations [9].

By application of voltage (or current), electrocoagulation (EC) process generates metallic ions, which associate with the OH^- produced at the cathode; the generated metal hydroxides have high sorption capacity, and favor the removal of impurities into solids that are referred to as flocs.

The simultaneous generation of cathodic gas (H_2) assists the electroflotation of the flocs [10]. EC process may be involved in the treatment of industrial wastewaters because of its simplicity and versatility; it is safe, operates under ambient conditions and it is not harmful to the environment [11]; it could be used [12] for efficient reducing or removing a large variety of pollutants from industrial effluents (food processing, textile industry, . . .). Moreover, EC appears efficient for the treatment of potable water [13],

* Corresponding author at: Laboratoire de Génie Chimique, Université Toulouse III-Paul Sabatier, Bât. 2RI, porte 126, 118, route de Narbonne, 31062 Toulouse Cedex 9, France.

E-mail address: tzedakis@chimie.ups-tlse.fr (T. Tzedakis).

¹ <http://lgc.cnrs.fr>, <http://www.univ-tlse3.fr/>, <http://www.fsi.univ-tlse3.fr>.

Nomenclature	
C_0 and C	Initial and temporal concentrations (kg/m^3)
COD	Chemical oxygen demand
E	Electrode potential (V) or electrical energy consumed per volume of the dye solution treated (kWh/m^3)
EC	Electrocoagulation process
EDTA	Ethylene Diamine Tetra Acetic Acid ($\text{C}_4\text{H}_4\text{N}_2\text{O}_4$) ⁴⁻
F	Faraday constant (96500 C/mol)
I, i	Applied current or applied current density (A or A/m^2)
IED	Inter-electrode distance (m)
ℓ	Solution thickness for absorption spectra (m)
k_j and $k_{app,j}$	Kinetic and apparent kinetic rate constant for specie j
K_j	Complexation or adsorption equilibrium constant for step j
M	Molar mass (kg/mol)
n_j	Mol number of the specie j
R^2	Correlation coefficient
RI	Ohmic drop of the electrolytic solution in the interelectrode space
SCE	Saturated calomel electrode
t	Time/duration of the electrolysis (s)
V	Volume treated of the waste solution (m^3)
CV	Crystal violet, or gentian violet, or triaryl-methane or $\text{C}_{25}\text{H}_{30}\text{N}_3\text{Cl}$, here also noted AN_3^+Cl^-
Z_{Al}	Al valence or the electrons exchanged number
Greek letters	
α, β	Stoichiometric factors and/or reaction kinetic orders
ΔV	Electrochemical cell voltage (V)
ε	Molar absorptivity or extinction coefficient ($\text{m}^3 \text{mol}^{-1} \text{m}^{-1}$)
η_a, η_c	Anodic and cathodic overvoltages (V)
λ	Wavelength (nm)
φ_c	Faradaic efficiency = $\frac{\text{loss in the Al mass}}{I_{\text{applied}} \times t \times M_{Al} / (3 \times F)}$
ϕ_v	$\frac{\text{Volume of the solution chemically treated in the bulk}}{\text{Interelectrodes volume}}$
χ	Ionic conductivity (S/m)

arsenic removal [14], fluorine removal from underground and waste waters [15], treatment of levafix orange textile dye solution [16], and alcohol distillery wastewater [17]. Zhian demonstrates that electrocoagulation allows decolorization of effluents containing heavy dyes like acid red 88 and leads to a removal efficiency close to 100% [18].

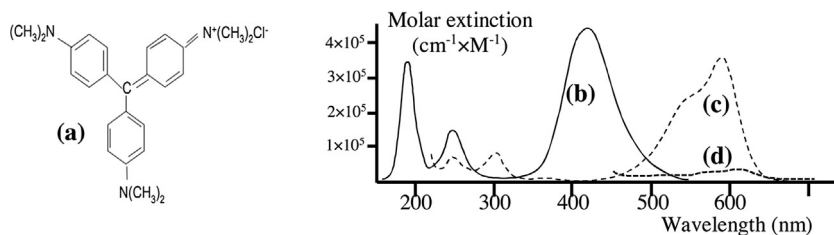


Fig. 1. (a) Structure of crystal violet; (b) absorption spectra for crystal violet in acidic solution [23]; (c) experimental absorption spectra for crystal violet in water [24]; (d) aqueous solution of the crystal violet containing NaCl 0.1 M after electrolyses (present study, various conditions).

Due to the complexity of the reactions in the electrocoagulation systems, the kinetic parameters of the various steps involved, are relatively difficult to determine, leading to uncertainties in the design and scale-up of industrial chemical reactors. To the best of our knowledge, kinetic modeling of electrocoagulation processes has been little investigated. Recently, Carmona has developed a model to predict the treatment of oil suspensions [19]; the adsorption equilibrium of organic matter on aluminum hydroxide was modeled using three kinetic equations. Lopicque propose a phenomenological model for treatment of industrial wastewater by electrocoagulation and based on global complexation equilibrium between $\text{Al}^{(\text{III})}$ species and the pollutants [20].

Ching-Yao Hu [21] proposes a variable order kinetic (VOK) model, derived from the Langmuir equation to express the kinetics of the fluoride removal reaction. The VOK model considers homogeneous kinetic aspects, adsorption isotherm and variation of the adsorbent mass during the electrocoagulation process; unfortunately, it uses adsorption isotherms laws 'at the equilibrium' to treat dynamic systems.

Kushwaha [22] applies electrocoagulation to treat dairy wastewater; it uses a 'multi-response' optimization technique to find the optimum values of operational parameters namely current density, pH, and provide values of the energy consumption associated to the COD abatement.

This present study investigates decolorization of the crystal violet (CV) dye solution by electrocoagulation method. CV is a cationic dye, widely used as a purple dye for textiles and also to dye paper [3]. The performances of electrocoagulation method to remove this dye have been evaluated using aluminum sacrificial anode as precursor of the coagulant. Furthermore, the effect of the various operating parameters has been experimentally optimized, and the results were applied i) to increase the knowledge of the mechanism of the overall process, and ii) to propose a model (associating electroregeneration and coagulation/complexation-adsorption) that could make reliable prediction of the efficiency of the electrocoagulation method at industrial scale.

2. Materials and methods

2.1. Characteristics of crystal violet

Crystal violet (CV) or gentian violet is a triarylmethane dye ($\text{C}_{25}\text{H}_{30}\text{N}_3\text{Cl}$, 407.98 g/mol, structure indicated in Fig. 1a). When dissolved in water ($\sim 4 < \text{pH} < \sim 10$), the dye has a blue-violet color with an absorbance maximum at 592 nm (Fig. 1c) with an extinction coefficient of $87000 (\text{mol L}^{-1})^{-1} \text{cm}^{-1}$; spectra recorded at various pH in this range (not provided here) show that the molar absorptivity does not significantly ($\Delta\varepsilon < 5\%$) changes against the pH. At pH 1.0, the dye is blue/green with absorption maxima at 420 nm and 620 nm, while in a strongly acidic solution ($\text{pH} = -1$), the dye is yellow with an absorption spectrum maximum at 420 nm (Fig. 1b).

Different colors are the result of the different charged states of the dye molecules. In the yellow form, all three nitrogen atoms carry a positive charge, while the green color corresponds to a form of the dye with two of the nitrogen atoms positively charged. At neutral pH, both extra protons are lost to the solution, leaving only one nitrogen atom positively charged [23,24].

CV hydrolyzes relatively slowly in alkaline media and results in the formation of the colorless carbinol, according to the kinetic law [25]:

$$-d[CV^+]/dt = (10^{-7} \text{ (s}^{-1}) \times a_{H_2O} + 0.194 \text{ (mol}^{-1}\text{s}^{-1}) \times [OH^-]) \times [CV^+] \quad \text{at } 298 \text{ K}$$

Nevertheless, for both the highest CV concentration and pH involved in this study, less than 0.1% of CV was hydrolyzed during the time of the runs, so this side reaction will be neglected.

2.2. Experimental-Apparatus-Electrodes reactions

All the electrocoagulation experiments were conducted using an undivided cell equipped with an aluminum and a stainless steel plates (2cm × 3cm × 2 mm for each) and the system operates in the batch mode (Fig. 2(i)). The electrolyzed volume is 0.1 L for all runs, and a VoltaLab PGZ 100 potentiostat was used to power the cell.

The effect of the various operating parameters was examined in the following domains:

- $3 \leq \text{pH}_{t=0} \leq 10$ (adjusted using NaOH or HCl and a Hanna pH-meter); $0.9 \leq \chi_{t=0, \text{ in mS/cm}} \leq 4.3$ (adjusted using a Hanna conductimeter and NaCl at concentrations ranging from 0.1 to 1 g/L, and also acting as supporting electrolyte);
- $100 \leq i_{\text{in A/m}^2} \leq 250$ (assuming an electro-active surface of $2 \times 0.02 \times 0.03 \text{ cm}^2$ for each electrode);
- $5 \leq [CV]_{t=0, \text{ in mg/L}} \leq 200$ (determined at 592 nm using an UV-visible 'Specord 250 Plus' device).
- $0.25 \leq \text{interelectrodes distance IED}_{\text{in cm}} \leq 1.5$;

After each experiment, electrolyzed solutions were filtrated (PTFE 13MM 0.45 μM/PP) and the dye removal efficiency $X = 1 - (VC)_{\text{after electr.}} / (VC)_{t=0}$ was estimated.

The spectroscopically determined concentrations of the residual dye in the electrolyzed solutions were periodically validated by the measurement of the chemical oxygen demand of the residual solution after filtration.

Aluminum, used as sacrificial anode, provides the Al^{3+} .



Water reduces on stainless steel cathode, producing gaseous hydrogen and hydroxide ions (R2).



According to the pH the electro generated Al^{3+} is converted into aluminum hydroxide (R3-a) and/or (R3-b), the coagulant used in EC [22,26].



Combination of reactions (R1) and (R3-a), leads to the overall electrochemical reaction (R4)



On the basis of this reaction scheme, the EC occurs globally, without changes neither of the pH, nor of the ionic strength in the bulk (far to the interelectrode space); nevertheless, these parameters change during the electrolysis close to the electrodes surfaces and significantly affect the EC performances.

The coagulant ($Al(OH)_{3(s)}$) interacts with charged (or not charged) species of dye and adsorbs them; in fact, during the EC process, CV contributes to neutralizing the surface charges of the dispersed particles of $Al(OH)_{3(s)}$, allows the reduction of the inter-particles repulsion, and thus enhances their agglomeration (the Van der Waals attraction predominates). The consequence is that flocs appear depending on the reaction (R5).



It is claimed that the EC limiting phenomenon which controls the pollutant removal, is its adsorption and entrapment into the aluminum hydroxide formed [27]; note that, the produced gaseous hydrogen contributes to bring flocs on the liquid surface enabling their flotation [26].

3. Results

3.1. Preliminary experiments

3.1.1. Anodic voltammograms obtained on the Al

Fig. 2(ii) presents typical current-potential curves obtained on aluminum anode. The curve (a) shows that in NaCl solution oxidation of the aluminum arises at $\sim -0.5 \text{ V/SCE}$. This potential decreases or around 250 mV in presence of CV, probably because a

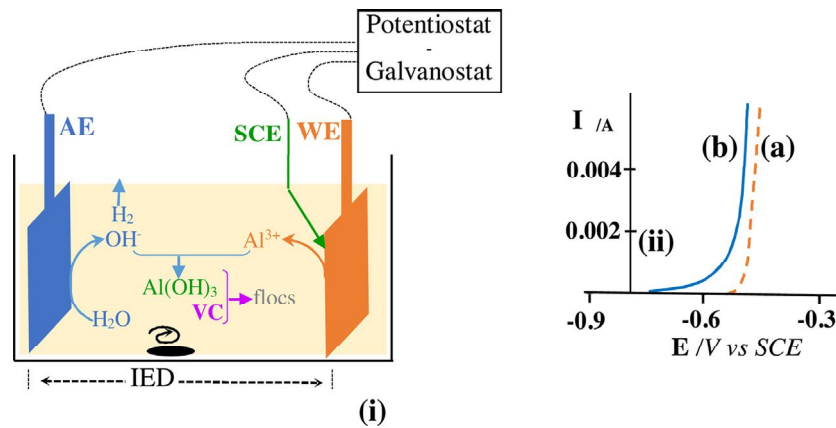


Fig. 2. (i): Schematic representation of the electrochemical reactor used to carry out EC studies; $0.25 \text{ cm} \leq \text{IED (interelectrode distance)} \leq 1.5 \text{ cm}$. (ii) current-potential curves obtained with the aluminum plate anode. $\text{pH}_{t=0} = 5.4$; $r = 0.3 \text{ V/min}$; (ii-a) NaCl 1 g/L; (ii-b) $[CV]_{t=0} = 0.1 \text{ g/L}$ in NaCl 1 g/L electrolyte.

certain complexation of the anodic products ($\text{Al}^{(\text{III})}$ and its oligomers, see next sections) by the dye. The consequence is that the CV facilitates the $\text{Al}^{(\text{III})}$ removal from the electrode and this imply that both the alumina formation and also the passivation/deactivation of the anode, were avoided.

3.1.2. EC preliminary runs-Effect of the pH

The pH is a key factor in electrochemical and chemical coagulation processes; under certain conditions, various complexes and polymeric compounds were formed via hydrolysis and polymerization reactions of the electrochemically dissolved $\text{Al}^{(\text{III})}$ [22,28–30].

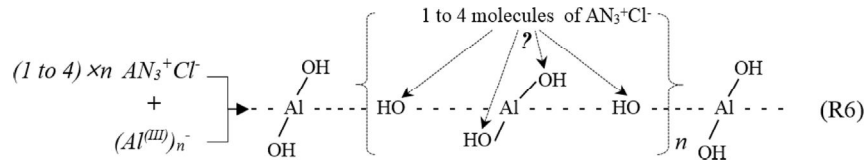
Hence EC experiments were conducted to study the effect of the pH on the CV removal; the results obtained, for an initial concentration of 100 mg/L, are shown in Fig. 3, which presents the temporal evolutions of both the residual free-CV concentration, and the pH (inset) during EC experiments.

Whatever the initial pH of the solution, it stabilizes at around 8.5 after 5 min of treatment. The water reduction (R2) does

characterized by their lower affinity i) to fix the CV, and ii) to be adsorbed on the existing flocs.

3.1.3. Reaction scheme for CV coagulation

The crystal violet structure has three nitrogens bearing free doublets that may act as electron donors to the aluminum hydroxide. Moreover, the quaternary protonated amino group could interact with oxygen of the negatively charged aluminum hydroxide particles. In addition, as previously mentioned [22,29,30], $\text{Al}^{(\text{III})}$ may react with OH^- to form various oligomeric species e.g. $\text{Al}_6(\text{OH})_{15}^{3+}$, $\text{Al}_7(\text{OH})_{17}^{4+}$, $\text{Al}_{13}(\text{OH})_{34}^{5+}$, to finally be transformed into an endless linked chain, structured as indicated in reaction (R6). This polymer $(\text{Al}(\text{OH})_3)_n$ acts as a coagulant and fixes CV molecules; consequently, one or more molecules of CV could interact with 1 molecule of aluminum hydroxide and the expected aim is to determine this number and also to evaluate how interaction occurs between CV and OH^- or CV and the $\text{Al}^{(\text{III})}$ atom. The following general scheme can be proposed (AN_3^+Cl^- represents the CV).



generates a constant production of hydroxides ions; they diffuse to the bulk and also to the anodic compartment, to precipitate the aluminum hydroxide; the initial period (~5 min) corresponds to the time required to establish the steady state between aluminum oxidation and aluminum hydroxide formation/polymerization, a step of which 'the steady state' pH appears to be 8.5; the electrocoagulation process is characterized by a buffer effect.

The CV concentration continuously decreases during 15 min' electrolysis, for all the pH; at a constant electrolysis time, for both initial pH values, lower than 5 or higher than 6, the crystal violet removal efficiency decreases. The optimum removal rate (65% at 15 min) was obtained for the natural pH (5.4) of the CV solution.

Note that, the Faradaic efficiency $\varphi_c = \frac{n_{\text{Al}^{(\text{III})}} \text{ really produced}}{n_{\text{Al}^{(\text{III})}} \text{ theoretically produced}} = \frac{\text{loss in the Al mass}}{i_{\text{applied}} \times t \times M_{\text{Al}} / (3 \times F)}$ was evaluated at the end of each experiment (by weighing the aluminum plate anode before and after treatment) and obtained values were higher than >95%.

The effect of the initial pH on the electrocoagulation process was related to the solubility of initially-formed aluminum hydroxide. At $\text{pH} < 5.4$ the $\text{Al}(\text{OH})_3$ is hydrolyzed and monomeric species ($(\text{Al}_\lambda(\text{OH})_{3\lambda-\mu}^{\mu+})$ such as Al^{3+} , $\text{Al}(\text{OH})^{2+}$, $\text{Al}(\text{OH})_2^+$ appear; they are able [29,30] to adsorb on particles that have (at the least at the beginning of the electrolysis) negative zeta potential [31], e.g. flocs of $\text{Al}(\text{OH})_3$, leading to charge neutralization. On the other hand, a decrease in the pH leads the ionic force to increase, implying that the electrical repulsion between $\text{Al}(\text{OH})_3$ particles decreases and these particles can coagulate; this leads to reduce their specific area as well as their interaction (adsorption capacity). These changes arise at the beginning of electrolysis ($t < 5$ min), but it is obvious that the produced adducts during this 'pH stabilization period', condition the feasibility/performance of the coagulation.

At pH ranging from 6 to 9 aluminum hydroxide precipitation arises; that may occur on the surface of aluminum hydroxide particles, or the hydroxide precipitates formed in the bulk, may attach themselves to the other particles. At pH values higher than 9, the aluminates ions, $\text{Al}(\text{OH})_4^-$, become the predominant species,

3.2. Experimental optimization of the operating parameters

Various EC runs were achieved, to determine the optimal operating parameters, allowing a rapid and low cost dye removal process to be proposed. Galvanostatic operations were carried out here, expecting to control the $\text{Al}^{(\text{III})}$ produced flux and also to overcome the cancellation of the current by an eventual passivation of the anode by an alumina deposit. Typical values

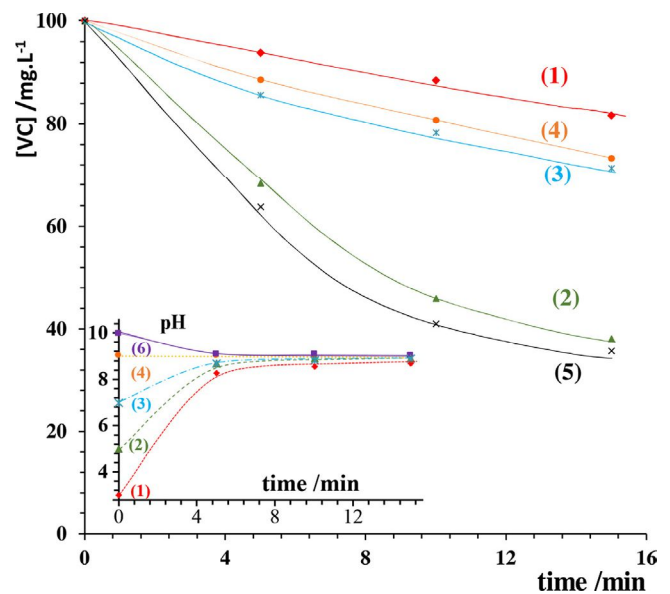


Fig. 3. Temporal evolutions of the residual free-CV concentration during EC runs on CV's aqueous stirred solutions. $[\text{CV}] = 0.1 \text{ g.L}^{-1}$; $\chi_{(\text{NaCl})} = 4.27 \text{ mS/cm}$; $i = 250 \text{ A/m}^2$; inter-electrode distance (IED) = 0.5 cm. Inset: Temporal evolutions of the pH for the same EC runs.

(1) \blacklozenge : $\text{pH}_{(t=0)} = 3.0$; (2) \blacktriangle : $\text{pH}_{(t=0)} = 5.0$; (3) \blackstar : $\text{pH}_{(t=0)} = 7.0$; (4) \bullet : $\text{pH}_{(t=0)} = 9.0$; (5) \times : $\text{pH}_{(t=0)} = 5.43$ (natural pH); (6) \blacksquare : $\text{pH}_{(t=0)} = 10.0$.

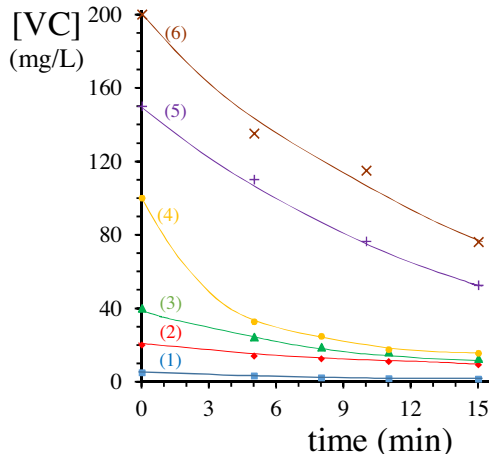


Fig. 4. Temporal evolutions of the residual concentration of the 'free' CV during EC operations carried out at various initial concentrations of CV. $i = 250 \text{ A/m}^2$; $\text{pH}_{t=0} = 5.4$. IED = 0.5 cm; Stirred solution; $\chi = 4.27 \text{ mS/cm}$; $[\text{CV}]_{t=0}$ in mg/L respectively: 1 ■; 5 ◆; 20 ▲; 40 ▲; 100 ●; 150 +; 200 X.

of the reactor voltage (ΔV) during electrolyses were in the range 5–15 V, as function of the applied current density, the CV concentration and the pH; furthermore this voltage may also be affected by the presence of both flocs and H_2 bubbles, both contribute to increase the electrical power dissipated under the Joule effect.

3.2.1. Effect of the initial concentration of the CV

Several 'fixed-duration' electrocoagulation experiments were achieved under galvanostatic conditions, varying the initial concentration of the CV, in the range 5–200 mg/L. The expected aims are i) to get information on the temporal decrease of the CV concentration in order to propose a coagulation simplified mechanism, ii) to deduce the equations describing the EC rate and to use them to model the system and to write a predictive tool for the dye coagulation rate. Fig. 4 indicates the temporal evolution of the residual concentration of the CV (spectroscopically determined as indicated above). For all runs this concentration

decreases over time, meaning that flocs were continuously created and precipitated.

To check if the adsorption step is slow and limits the overall process, simplified kinetic analysis was performed, considering the reaction (R5) as a simple reaction obeying to the Van t'Hoff laws, and assuming the quantity of the produced $\text{Al}(\text{OH})_3$ to be constant (even if it is continuously produced by the anode oxidation) and without effect on the coagulation rate.

The integration of the kinetic equation (E1) of the reaction (R5), provides the temporal evolution of the residual concentration of CV in the suspension

$$-(1/\beta) \frac{dC}{dt} (\text{in mg/L/min}) = k \times C^\beta (\text{in mg/L}) \times [\text{Al}(\text{OH})_3]^\alpha (\text{in mg/L}) \quad (\text{E1})$$

None, neither first ($\ln[\text{CV}] = f(t)$), nor the second ($1/[\text{CV}] = f(t)$) or third ($1/[\text{CV}]^2 = f(t)$) kinetic orders correctly fit the experiments for the various runs (results not showed). This indicates that complexation (or adsorption) kinetic was not the only limiting phenomenon, electrogeneration of the Al^{3+} and/or production of the corresponding oligomers/polymers of the aluminum hydroxide also limit the overall process. This fact was also claimed by Mameri, which shows that in the electrocoagulation process, the concentration of the produced $\text{Al}^{(\text{III})}$ is a limiting factor for the formation of flocs [32]. For example in the case of the removal of fluoride from drinking water ($i = 200 \text{ A/m}^2$) the adsorption reaction (complexation in fact to AlF_6^{3-}) is rapid! A more complete theoretical analysis of these experiments will be performed in the next sections.

3.2.2. Effect of the inter-electrode distance (IED)

For EC processes carried out under galvanostatic conditions, the IED does not affect (theoretically) the produced flux of $\text{Al}^{(\text{III})}$, it affects the required voltage and consequently the energy consumption for electrolysis, especially when the conductivity is low. Fig. 5 shows experimental results of the temporal evolution of the CV removal rate against the IED in the range of 0.25–1.5 cm; for all electrolyses the residual concentration of CV decreases in the bulk; furthermore, at constant electrolyses times, the CV removal rate versus the IED (or also versus the ratio $\phi_v = \frac{\text{Volume of the solution 'chemically' treated in the bulk}}{\text{Inter-electrodes volume}}$) exhibits peak-shaped curves (Fig. 5b), which present a maximum for an IED from 0.5 to 0.6 cm (or a ϕ_v from 30 to 35). In addition to the effect on the

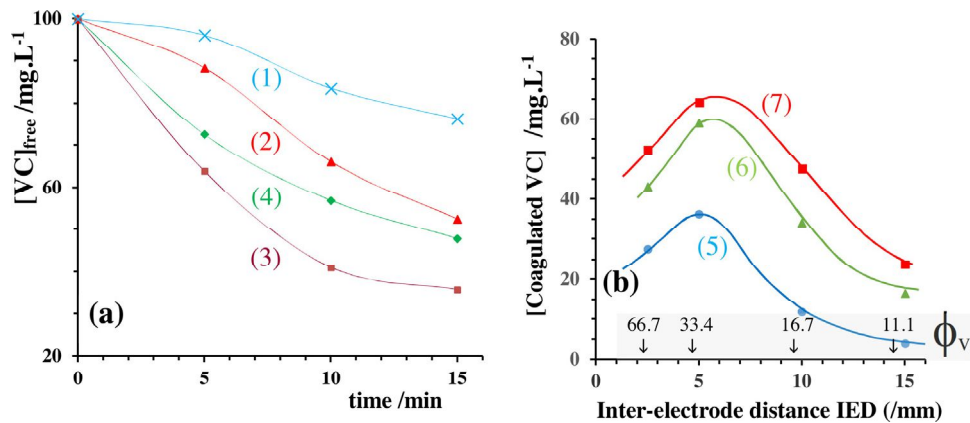


Fig. 5. Results of EC runs on 'CV's aqueous stirred solutions' carried out at various IED. $[\text{CV}] = 100 \text{ mg/L}$; $\chi_{\text{NaCl}} = 4.27 \text{ mS/cm}$; $\text{pH}_{t=0} = 5.4$; $i = 250 \text{ A/m}^2$. (a): temporal evolution of the residual concentration of the CV free in the bulk; IED respectively in cm: (1) X; 1.5; (2) ▲; 1.0; (3) ■; 0.5; (4) ◆; 0.25. (b): Coagulated concentration of CV dependence on the interelectrode distance (or the volumes ratio ϕ_v), for constant electrolyses durations (results extracted from, a). (5) ●; 5 min, $[\text{CV}]_{\text{coagulated}} (\text{mg L}^{-1}) = 3.10^{-3} \times \phi_v^3 - 0.002 \times \phi_v^2 + 1.965 \times \phi_v - 18.8$. (6) ▲; 10 min, $[\text{CV}]_{\text{coagulated}} (\text{mg L}^{-1}) = 6.10^{-3} \times \phi_v^3 - 0.112 \times \phi_v^2 + 5.971 \times \phi_v - 38.3$. (7) ■; 15 min, $[\text{CV}]_{\text{coagulated}} (\text{mg L}^{-1}) = 8.10^{-3} \times \phi_v^3 - 0.125 \times \phi_v^2 + 6.195 \times \phi_v - 28.4$.

energy consumption, the IED also affects the stirring of the solution located between the anode and the cathode, and consequently the uniformization of the operating parameters. For low IED distances (0.25 cm), the dispersion of the flocs from the IED space to the bulk, appears more difficult, flocs remain in the IED and cause side-reactions (for ex. accumulated hydrogen oxidation on the Al anode) to take place, leading to the decrease in the CV removal rate.

For IED greater than 0.5 cm, a decrease in the CV removal rate is due to a longer time required for electrogenerated $\text{Al}^{(\text{III})}$ to meet OH^- ions and to react with them (longer distance to diffuse) thus different forms of oxygenated aluminum could be produced and these forms were less active against the adsorption of the CV. Another explanation could be the hydrogen fraction (lower for $\text{IED} > 0.5$ cm), is not sufficient to favor the removal of flocs from the interelectrode space; indeed, according to the studies of Prasinidis [33,34], the size distribution of the flocs is strongly conditioned by the shear-rate of the solution; in a stirred batch reactor, increasing the shear-rate amplitude causes the average floc size (obtained at the steady state e.g. balance between coagulation and dispersion) to decrease. In the present study, increasing IED enhance stirring of the solution between the two plates which is fatal to the creation of flocs.

3.2.3. Effect of the current density

Current density i determines the production of both the coagulant flux and the hydrogen bubbles, conditioning thus the size and growth of the flocs and consequently the efficiency of the EC. Fig. 6(a) shows the experimental results of EC runs, carried out under various current densities from 100 to 250 A/m^2 . At a constant i the residual concentration of CV decreases over time. Moreover for a constant electrolysis duration, this concentration also decreases when the applied current increases.

For reaction times of 15 min, the coagulated concentration of CV increases from 19 to 65% when i increases from 100 to 250 A/m^2 , which corresponds to the expected behavior ($i \uparrow$, flux of $\text{Al}^{(\text{III})} \uparrow$, $[\text{CV}]_{\text{free}} \text{ decreases}$). Fig. 6-b (extracted from 6-a), shows the dependence of the coagulated concentration of the CV, for constant electrolyses times versus the applied current density; curves exhibit a no linear evolution. Oxidation of aluminum takes place under activation limitation, there are neither nor mass transfer limitation nor side reactions (no oxidation of water, nor for chloride; the complexation of $\text{Al}(\text{III})$ by CV does not introduce limitation but accelerate the reaction). This implies that the whole applied current was used to oxidize Al. Assuming the coagulation as ‘instantaneous’ (and also limitation of the process caused by the

Al oxidation) then, it would be expected a linear correlation $[\text{CV}]_{\text{in the flocs}} = f(i)$, exhibiting a slope equal to one. The ‘no-linear’ variation obtained (see equations on the caption) clearly demonstrates that the coagulation reaction (R5) is not instantaneous; limitation of the overall process, caused by both the anodic generation of the adsorbent and also by its coagulation reaction. Furthermore, curves $[\text{Coagulated CV}] = f(i)$ could be assumed as linear for $i > 100 \text{ A}/\text{m}^2$; in this case they exhibit slopes higher than 1, demonstrating that the $\text{Al}^{(\text{III})}$ cumulates in the bulk before being saturated (adsorption) by the crystal violet.

3.2.4. Effect of the initial ionic conductivity

Sodium chloride is used to regulate the conductivity of the solutions to be treated by electrocoagulation. Fig. 7 shows the results obtained for various electrocoagulation sets, performed using NaCl concentrations in the range of 0.2–1.0 g/L under galvanostatic conditions. The residual concentration of the CV, free in the bulk, decreases over time for all the experiments (Fig. 7(a)), more significantly for higher conductivities.

Furthermore, at constant durations of electrolysis, this concentration also decreases when the conductivity of the solution increases and these results clearly indicates a strong dependence of the ionic conductivity on the dye coagulation rate. As an example, for 15 mins’ electrolysis, the coagulated concentration of CV increases from 35 to 65% when χ increases from 0.9 to 4.3 mS/cm . (Fig. 7(b)). Canizares study the electrodisolution of aluminum electrodes in electrocoagulation processes, and claims a ‘strong influence of the pH’ and ‘no influence of the supporting electrolyte’ on the dissolution of Al which appears to solely depend on the amount of charge passed [35]. In the present study, the initial pH was adjusted, and the enhancement in the removal of the dye was only due to the increase of the chloride concentration.

Several assumptions could be proposed to explain the dependence of the removal rate to the ionic conductivity. Decreasing the electrolyte concentration enhance the migration flux of the charged species (CV, OH^- , and also of the $\text{Al}^{(\text{III})}$ adducts).

CV will move to the cathode and the ‘negatively charged particles of the aluminum hydroxide’ (i.e. oligomers, polymers and flocs) move to the anode. Moreover, the mobility values of these species are very different (solid particles have weak negative zeta potential, in comparison with the positive charge of the nitrogen in the CV) and the consequence is in fact their rapid separation, instead their rapprochement.

In addition, formation of the aluminum precipitates requires OH^- , which comes from the cathode by diffusion, by convection,

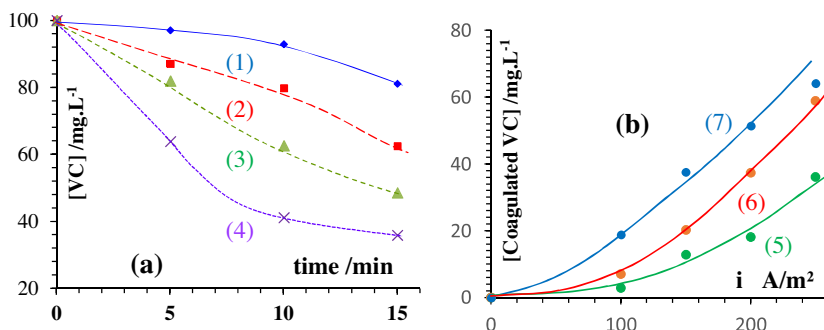


Fig. 6. Results of EC operations on CV's aqueous stirred solutions, carried out at various current densities. $[\text{CV}]_0 = 100 \text{ mg L}^{-1}$; $\chi_{\text{NaCl}} = 4.27 \text{ mS}/\text{cm}$; $\text{pH} = 5.43$; $\text{IED} = 0.5 \text{ cm}$. (a): residual concentration of the CV free in the bulk against the time. $i (\text{A}/\text{m}^2)$ respectively: (1) \blacklozenge : 100; (2) \blacksquare : 150; (3) \blacktriangle : 200; (4) \times : 250. (b): Applied current density dependence on the coagulated concentration of the CV, for constant durations of electrolysis (results extracted from Fig. 6, a). (5) \blacksquare : 5 min $\{[\text{CV}]_{\text{in the flocs}}\} = 0.7 \cdot 10^{-3} \times i^2 + 0.019 \times i$, $R^2 = 0.99$; (6) \bullet : 10 min $\{[\text{CV}]_{\text{in the flocs}}\} = 10 \cdot 10^{-4} \times i^2 + 0.013 \times i$, $R^2 = 0.99$; (7) \blacktriangle : 15 min $\{[\text{CV}]_{\text{in the flocs}}\}_{\text{mg/L}} = 3 \cdot 10^{-4} \times i^2 + 0.188 \times i$, $R^2 = 0.99$; see units of I and C on the plot.

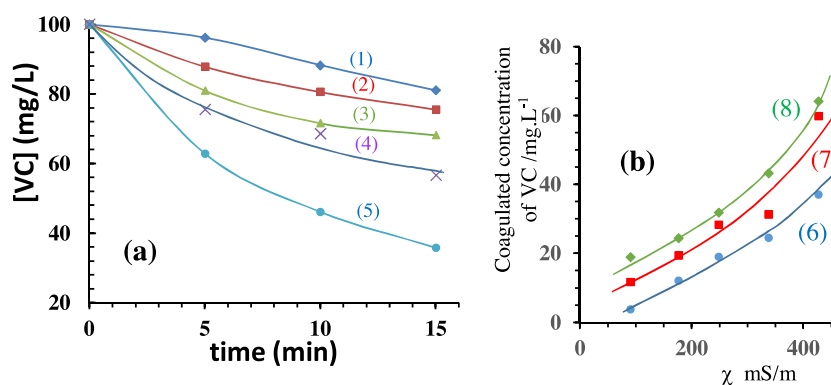


Fig. 7. Results of EC operations on 'CV's aqueous stirred solutions' carried out under galvanostatic conditions at various initial conductivities. $[CV]^\circ = 100 \text{ mgL}^{-1}$; $\text{pH}_{\text{adjusted at } t=0} = 5.43$; $\text{IED} = 0.5 \text{ cm}$. (a): residual concentration of the CV free in the bulk against the time. $[\text{NaCl}]^\circ (\text{g L}^{-1})$ and $\chi (\text{mS/cm})$ respectively: (1) \blacklozenge : 0.2 and 0.9; (2) \blacksquare : 0.4 and 1.76; (3) \blacktriangle : 0.6 and 2.48; (4) \times : 0.8 and 3.38; (5) \bullet : 1.0 and 4.27. (b): Ionic conductivity dependence on the concentration of the coagulated CV, for constant electrolyses durations (extracted from Fig. 7, a). (6) \bullet : 5 min; $[\text{CV}_{\text{in the flocs}}] = 6.10^{-5} \times \chi^2 - 63.10^{-3} \times \chi + 0.95$, $R^2 = 0.99$; (7) \blacksquare : 10 min; $[\text{CV}_{\text{in the flocs}}] = 20.10^{-5} \times \chi^2 - 10.10^{-3} \times \chi + 10.1$, $R^2 = 0.99$; (8) \blacklozenge : 15 min; $[\text{CV}_{\text{in the flocs}}] = 30.10^{-5} \times \chi^2 - 20.10^{-3} \times \chi + 18.6$, $R^2 = 0.99$; see units of χ and C on the plot.

and as function of the Cl^- concentration, by migration. Increasing the OH^- migration flux, appears to be favorable to the aluminum hydroxide formation but unfavorable to the coagulation (CV/solid aluminum hydroxide particles), because to high migration flux of the CV to the cathode.

Note that, at constant current density, the decrease in salt concentration requires to increase the supplied cell voltage (ΔV) and consequently to increase the power consumption in the electrolytic cell; typically, increasing conductivity from 0.9 to 4.43 mS/cm causes the operating voltage (ΔV) to decrease from $\sim 12 \text{ V}$ to $\sim 5 \text{ V}$. Nevertheless, for the lower ionic conductivity, the dissipated power remains low, ($6.10^{-4} \text{ m}^2 \times 250 \text{ A/m}^2 \times 12 \text{ V} = 1.8 \text{ W}$ for 100 cm^3 of solution) and does not lead to a significant change in temperature of the solution; this fact excludes the temperature influence for these EC runs.

In addition, an increase in the chloride concentration has two supplementary consequences, probably less important than the previous one:

- the complexation of electrogenerated aluminum by an excess of chloride (to leads of adducts such as AlCl_x^{3-x}) could also affects the formation of the polymeric chain acting as flocculent;
- the augmentation of the ionic force, leading to the declining of the interactions between the aluminum hydroxide particles, and promoting their coagulation.

To sum up, even these results need a deeper analysis, they show that concentration of chloride favors the CV removal and a compromise has to be chosen in order to avoid the rejection of high salinity concentrations after dye removal.

3.3. Theoretical analysis of the system 'anodic oxidation/coagulation of the CV'—Proposed reaction scheme and discussion

This section develops a simplified model, based on the complete system: electrochemical oxidation coupled to the CV coagulation, and expecting to provide the simulated temporal evolution of the CV concentration, obtained on the basis of a proposed reaction mechanism.

The following assumptions were made: the coagulant ($\text{Al}^{(\text{III})}$) is continuously electrogenerated, so the system cannot reaches the equilibrium (of complexation or adsorption) before cancellation of the concentration of the CV. The overall mechanism of the decolorization was assumed here to include reactions (R1), (R3-a) and (R5).

According to Faraday's law, the real mole number of the produced aluminum, under a constant applied current (I_{applied}) during time t is:

$$n_{\text{Al}^{(\text{III})} \text{ really produced}} = \phi_c \frac{I_{\text{applied}} \times t}{z_{\text{Al}} \times F} = \frac{\text{mass}_{\text{Al}}}{M_{\text{Al}}} \quad (\text{E2})$$

where: ϕ_c the faradaic efficiency; F the faraday constant and z_{Al} the Al valence.

This quantity could be present in the following four forms in the bulk:

$$n_{\text{Al}^{(\text{III})} \text{ really produced}} = n_{\text{Al}^{3+} \text{ free}} + n_{\text{Al}(\text{OH})_3 \text{ oligomer(s) free}} + n_{\text{Al}(\text{OH})_3 \text{ dissolved}} + n_{\text{Al}(\text{OH})_3 \text{ in flocs}} \quad (\text{E3})$$

At the operating pH ($3.5 < \text{pH} < 10$), both the quantities of free Al^{3+} and free dissolved $\text{Al}(\text{OH})_3$ can be neglected ($\log [\text{Al}(\text{OH})_3 \text{ dissolved}] \leq -2$) [22,26].

Taking these assumptions into account, the mole number of the $\text{Al}(\text{OH})_3$ free in the bulk can be expressed as follows:

$$n_{\text{Al}(\text{OH})_3 \text{ oligomer(s) free}} = \phi_c \frac{I_{\text{applied}} \times t}{z_{\text{Al}} \times F} - n_{\text{Al}(\text{OH})_3 \text{ in flocs}}$$

The dissolved residual crystal violet moles number = $n_{\text{CV free in the bulk}} = n_{\text{CV}}^\circ - n_{\text{CV in flocs}}$

Assuming that α moles of $\text{Al}(\text{OH})_3$ reacts with β moles of CV, the moles number of $\text{Al}(\text{OH})_3$ in the flocs can be expressed as: $n_{\text{Al}(\text{OH})_3 \text{ in flocs}} = \frac{\alpha}{\beta} n_{\text{CV in flocs}}$.

And the $n_{\text{Al}(\text{OH})_3 \text{ oligomer(s) free}} = \phi_c \frac{I_{\text{applied}} \times t}{z_{\text{Al}} \times F} - \frac{\alpha}{\beta} \times (n_{\text{CV}}^\circ - n_{\text{CV free in the bulk}})$

The kinetic equation of the reaction (R5) can be expressed as follows:

$$\frac{dn_{\text{CV free in the bulk}}}{\beta V dt} = k_6 \times \left(\frac{n_{\text{Al}(\text{OH})_3 \text{ oligomer(s) free}}}{V} \right)^\alpha \times \left(\frac{n_{\text{CV free in the bulk}}}{V} \right)^\beta \quad (\text{E4})$$

Taking into account the previous established molar quantities, this equation can also be written as:

$$d \frac{[\text{CV free in the bulk}]}{dt} = -\beta \times k_6 \times \left(\phi_c \frac{I_{\text{applied}} \times t}{Z_{\text{Al}} \times F \times V} - \frac{\alpha}{\beta} \times (C^\circ - [\text{CV free in the bulk}]) \right)^\alpha \times [\text{CV free in the bulk}]^\beta$$

simplified as:

$$\frac{dC}{dt} = -\beta \times k_6 \times \left(\phi_c \frac{I_{\text{applied}} \times t}{Z_{\text{Al}} \times F \times V} - \frac{\alpha}{\beta} \times (C^\circ - C) \right)^\alpha \times C^\beta \quad (\text{E5})$$

Where C and C° : The temporal and the initial concentrations of dissolved CV (mg/L) assumed to be present under the mono-protonated form.

The analytical solution of this equation, for the simpler kind of $\alpha = \beta = 1$, was available, but here the Euler method $\{(dC/dt=f(C,t); C_{j+1} = C_j + \text{step} \times f(C_j, t_j))\}$ was used to solve it; four different kinds were treated: i) $\alpha = \beta = 1$; ii) $\alpha = 1$ and $\beta = 2$; iii) $\alpha = 1$ and $\beta = 3$; iv) $\alpha = 1$ and $\beta = 4$, for respectively 1, 2, 3 or 4 molecules of CV fixed on 1 molecule of $\text{Al}(\text{OH})_3$, as indicated in (R6). Nevertheless, the electrocoagulation reaction (R5) appears more complex than an elementary reaction, obeying to the Van t'Hoff laws. Here we will assume that, even if coagulation takes place in several steps or with several solid adducts (oligomers), the rate-determining step involves one unit of solid aluminum hydroxide (alone or constituting a part of an oligo/polymeric chain) which contains various interaction sites and simultaneously interacts with molecules of the crystal violet. Binding or adsorption on multilayers was not considered, because our assumption involves chemical interactions between the protonated nitrogen of CV and oxygen (R6) and this assumption excludes multiple/overlay chemical bounds.

Iterative calculations were achieved to determine the value of the kinetic constant k_6 that enables getting the best fit between experiments and simulation for each one of the four examined combinations of the kinetic orders.

Results were presented in Fig. 8, which compares the theoretical curves of the temporal evolution of the crystal violet concentration, with the experimental results (Fig. 4). Note that the curves do not contain experimental points for less than 5 min electrolyses, because during this period the pH changes.

Plots A-i to A-iv present calculations achieved with a fixed $[\text{CV}]^\circ = 40 \text{ mg/L}$. Each plot provides the value of the kinetic constant k_6 that enable obtaining the best fit for the indicated combination of the orders α and β . Analysis of these plots indicates that only the combination $\alpha = 1$, $\beta = 4$ (plot A-iv), enables correctly fitting the theoretical with the experimental curves, for a value of k_6 equal to $7.10^{-7} \text{ L}^4 \times \text{min}^{-1}/\text{mg}^4$; for all other examined order's combinations, no value of k_6 allows any satisfactory correlation between the theoretical and the experimental results.

Based on these results, it can be deduced that the electrocoagulation reaction (R5 or R6) involves 1 unit of aluminum hydroxide and 4 molecules of CV. Because the pH of all the solutions stabilizes at 8.5 after a few minutes of electrolysis (Fig. 3 inset), the more abundant form of CV in solution is the protonated form, it can be considered that these interactions occur between the protonated nitrogen and oxygen (4 molecules of VC in reaction R6).

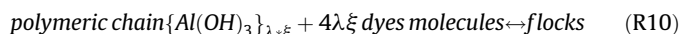
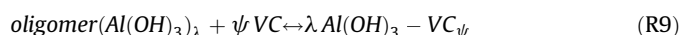
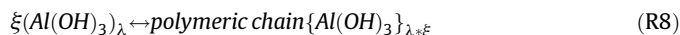
The determined kinetic rate $\left(\frac{dC}{dt} = -\beta \times k_6 \times \left(\phi_c \frac{I_{\text{applied}} \times t}{Z_{\text{Al}} \times F \times V} - \frac{\alpha}{\beta} \times (C^\circ - C) \right)^\alpha \times C^\beta \right)$ was validated for all the examined concentrations of CV in Fig. 4, but (for simplicity) only results for four concentrations (plot and optimum value of k_6) were reported in Fig. 8, B-i to B-iv; the agreement between theoretical and experimental results is satisfactory for all the

examined cases. Note that the effect of all the combinations of the kinetic orders was examined and the temporal evolution of the CV concentration was represented (e.g. curves/straight lines on the top of each plot), even if results of combinations $\alpha = \beta = 1$; $\alpha = 1$, $\beta = 2$; $\alpha = 1$, $\beta = 3$ are no satisfactory.

The values obtained for the kinetic constant k_6 appear to be dependent on the initial concentration of CV. The plot of Fig. 8 (C) provides the logarithmic evolution of the theoretical value of k_6 (iteratively determined, for $\alpha = 1$, $\beta = 4$ and each CV initial concentration), as a function of the initial concentration of the CV.

$$k_6 = 1.107 / ([\text{CV}]^\circ)^{-4} \quad (\text{E6})$$

The linear correlation obtained (caption of Fig. 8), leads to the equation (E6) which provides the dependence of the k_6 with the initial concentration of CV. Increasing the initial concentration of the crystal violet leads the electrocoagulation rate to decrease by 'four orders'. Following these results it may be proposed a more realistic reaction mechanism than this used for simulation: For $\text{Al}(\text{OH})_3$ production, reactions (R2) and (R3-a) were considered. Alumina formation was excluded on the basis of §3-1-1, Fig. 2, ii.



The decrease in the kinetic constant with the initial violet concentration could be due to the following reasons:

- Aluminum hydroxide molecules creates oligomers (R7) before becoming a long polymeric chain (R8) these oligomers react with the CV (one or more molecules/Al atom), depending on the reaction (R9) but the resulting complexes do not easily associate to create flocs, thus increasing the CV concentration favors the reaction (R9) and disadvantages the reaction (R10). Reaction (R10) assumes that the main process involves according: first the creation of the polymeric chain of the coagulant, and secondly the interaction with the dye molecules.
- Adsorption isotherm models were used classically to describe electrocoagulation; nevertheless, interactions between CV and aluminum hydroxide could be considered as complexation type reactions. If the analogy with the adsorption of CV on the aluminum hydroxide could be made, we suggest the following mechanism to explain the dependence of k_6 on the CV initial concentration: Existence of at least four different oligomers of the aluminum hydroxide [22] and interactions of the CV with each oligomer (R9). Assuming 'a unique interaction' between the CV and each oligomer, followed by the association of the resulting complexes 'oligomer-CV' (assumed as the step controlling the overall rate) leading to the flocs creation, then the equation (E7) could be put forward to describe the overall coagulation rate [36].

$$r = k \times K_1 \times K_2 \times K_3 \times K_4 \times (n_{\text{Al(III)}}/V) \times [\text{CV}]^4 / \{(1 + K_1[\text{CV}]) \times (1 + K_2[\text{CV}]) \times (1 + K_3[\text{CV}]) \times (1 + K_4[\text{CV}])\} \quad (\text{E7})$$

where: K_j and k are respectively the complexation constant of the association of the oligomer j with the CV and the kinetic constant of the reaction of the complexes 'oligomers-CV' to create flocs.

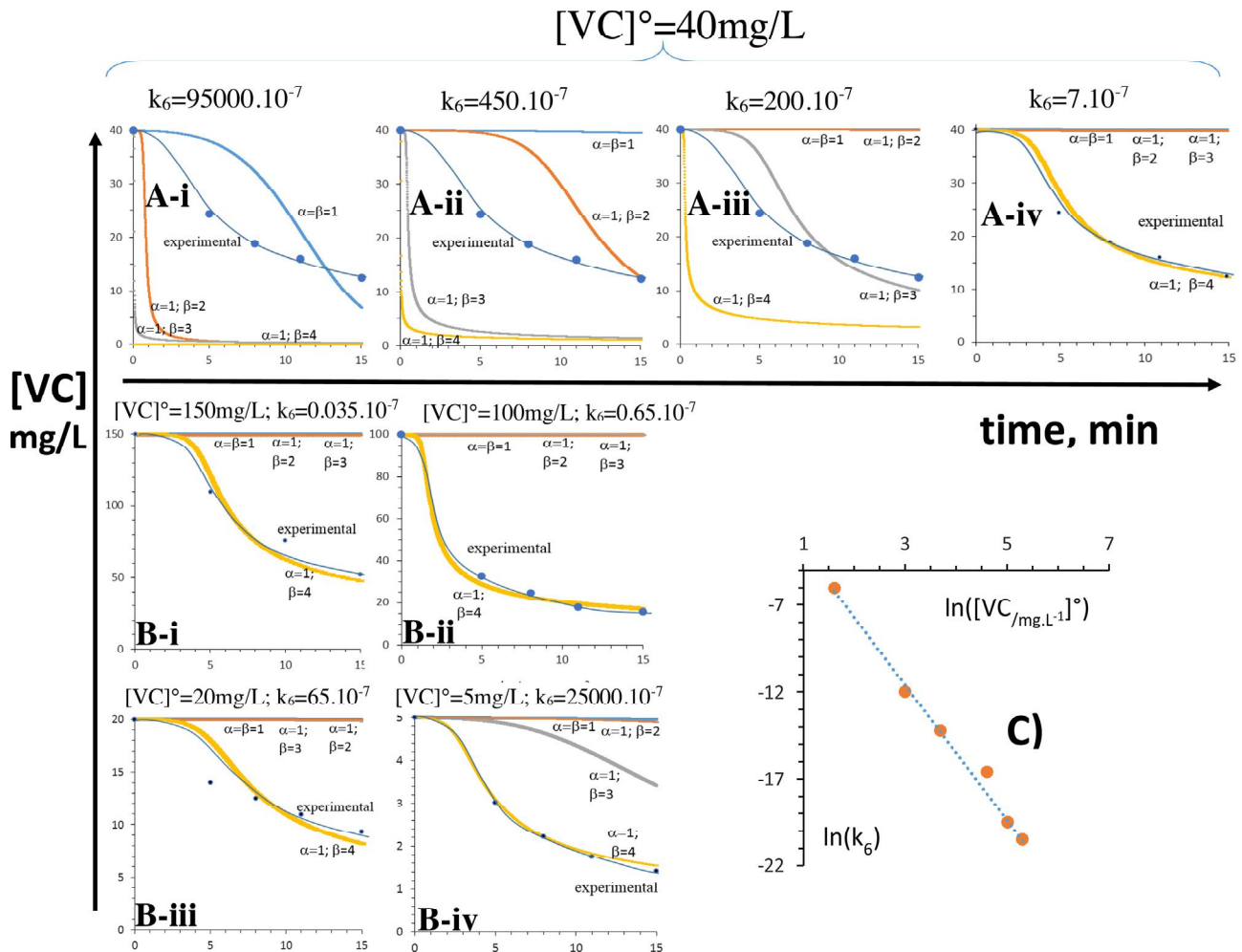


Fig. 8. Comparison between simulated and experimental results.

Top: $[CV]^\circ = 40 \text{ mg/L}$: (A-i) $\alpha = \beta = 1$; (A-ii) $\alpha = 1$; $\beta = 2$; (A-iii) $\alpha = 1$; $\beta = 3$; (A-iv) $\alpha = 1$; $\beta = 4$.

Bottom, B-i to B-iv: $[CV]^\circ$ in the range of 150–5 mg/L. Optimal value of k_6 for $\alpha = 1$; $\beta = 4$.

Bottom C: Logarithmic evolution of the iteratively determined k_6 versus the initial concentration of the CV (for all the $[CV]^\circ$ examined in Fig. 4); $\ln k_6 = -3.899 \times \ln [CV]_{\text{mg.L}^{-1}} + 0.1018$; $R^2 = 0.998$.

This mechanism could be reasonably considered, since the floc-size distribution requires sufficient time to reach steady state (reflecting the balance between coagulation and fragmentation [33,34]); furthermore the floc-size distribution is strongly conditioned by the applied shear rates, here controlled by the IDE (or ϕ_v), the H_2 production rate (thus the applied current) and the stirring of the solution.

As a function of the complexation constant K_j values (or the coverage ratio if adsorption instead complexation is considered), the equation (E7) may be simplified and lead to an inversely proportional relation between the kinetic constant (k_6) and the exponent 4 of the CV concentration, which justifies the obtained relation (E6).

Indeed, assuming significant affinity of the CV against the oligomers, each term in the denominator can be simplified by only keeping the product $K_j[CV]$ and neglecting 1; thus equation (E7) becomes $r = \{k/[CV]^4\} \times (n_{Al(III)}/V) \times [CV]^4$, where the term $\{k/[CV]^4\}$ was previously assumed as constant (k_6) for the iterative calculations. In this assumption, the term $\{k/[CV]^4\}$ is of course 'no constant' during the coagulation advancement/decrease of the CV concentration, and this could partially explain the exponent 3.8 instead of 4.

3.4. Cost of the EC treatment

The electrical energy and the electrode material have been taken into account as a major part in the calculation of the operating cost, comparatively to the cost of chemicals, and the simple separations steps required (sludge dewatering and disposal).

Typical values are:

- the electrical energy required to remove 70% of CV at 100 mg/L from 0.1L waste solution:

$$E_{(kWh/m^3)} = \Delta V \times I \times \text{time} / (X_{EC} \times [CV]_{\text{kg/L}}^\circ \times V) = 27 \text{ kWh/kg of CV in } 10 \text{ m}^3 \text{ of waste solution, a value which can be reduced using a more sophisticated reactor.}$$

- cost of Al consumed to treat 10 m^3 of waste solution containing 0.1 g/L of CV:

$$\text{Al price} \times I \times \text{time} \times M_{Al} / (z_{Al} \times F \times X_{EC} \times [CV]_{\text{kg/L}}^\circ \times V) \sim 9 \text{ US \$/kg of CV}$$

- sludge produced: 1.79 kg of Al flocs containing 1 kg of CV and salinized water, and this step requires a simple 'macro-filtration' operation.

Note that this process produces gaseous hydrogen constituting a valuable product.

4. Conclusion

This study was a first step to improve the knowledge regarding the mechanism and the modeling of the kinetics of crystal violet removal by electrocoagulation using aluminum as sacrificial anode and stainless steel as cathode. The EC method applied in this study provides a sensitive, rapid and reliable technique for the removal of the CV. Its effectiveness was indeed demonstrated for initial concentrations of CV in the range from 5 to 200 mg/L; a color reduction greater than 70% (simultaneous to the organic matter corresponding decrease) was observed for 15 min' electrolyses and a complete removal was obtained for reaction times of about 1 h. The experimental optimization of the system allows the selection of the required operating parameters to maximize the removal yield; in particular the current density (250 A/m²), the inter-electrode distance (0.5 cm) and the ionic conductivity regulated by the NaCl concentration (1 g/L). Note that a surprising result (we are not able to rigorously explain its physical meaning at this time) concerns the pH effect: even if after few minutes (3–5 min) of electrolysis, the pH of the solution stabilizes to around 8.5, the initial pH of the CV solution significantly influences the electrocoagulation rate as well as its removal yield, optimal values being obtained at the natural pH = 5.4. Both the acid/base equilibria and the initial kinetics of the Al(OH)₃ polymerization could be significantly affected by the initial pH of the waste and disadvantage the process performances.

Simple kinetic analyses clearly demonstrate that fixation of the CV (complexation/adsorption) is not a unique phenomenon which conditions the electrocoagulation rate; electrogeneration of Al^(III) and a certain polymerization of the aluminum hydroxides also affect this process.

A more complete theoretical analysis, that correlate well with experiments, has demonstrated that in the coagulation reaction 4 molecules of CV associate (mainly by chemical binding than physical adsorption) with one unit of the aluminum hydroxide contained within oligo/poly-meric chains.

This study demonstrates that the association of CV with various oligomers of the coagulant was also possible and contributes to reduce the overall rate of the EC process. At this stage of the investigation, the simple proposed model, taking into account the applied current and the CV concentration, enables the prediction of the temporal evolution of the coagulated dye and its removal rate. Furthermore, a deeper investigation is required to model the effect of both the pH and ionic conductivity, and this will constitute the next step of this study.

To sum up direct extrapolation of this chipper process on an industrial scale could be easier to carry out; moreover this same approach can be used for the treatment of other dyestuffs or in general for the modeling of any electrocoagulation process.

Acknowledgements

The authors would like to thank: i) the Ministry of National Education and Research of the Republic of Senegal for financially supporting this research under Impulse Fund for Scientific and Technical Research; ii) the Paul Sabatier University (UT III Toulouse) for financially supporting this research at the chemical engineering laboratory; iii) Thanks are also due to Sophie Chambers for checking the manuscript.

Appendix A. Supplementary data

Supplementary data associated with this article can be found, in the online version, at <http://dx.doi.org/10.1016/j.jece.2016.09.002>.

References

- [1] P. Sine, *Synthetic Dyes*, West Ed. Rajat Publications, New Delhi, 2003.
- [2] N. Daneshvar, A.R. Khataee, N. Djafarzadeh, The use of artificial neural networks (ANN) for modeling of decolorization of textile dye solution containing C.I. Basic Yellow 28 by electrocoagulation process, *J. Hazard. Mater.* B137 (2006) 1788–1795.
- [3] D. Ghosh, C.R. Medhi, H. Solanki, M.K. Purkait, Decolorization of crystal violet solution by electrocoagulation, *J. Environ. Prot. Sci.* 2 (2008) 25–35.
- [4] S.K. Dubey, P. Srivastava, A. Verma, R. Anita, Solar photo-catalytic treatment of textile wastewater for biodegradability enhancement, *Int. J. Environ. Eng.* 1 (2) (2009) 152–164.
- [5] R.K. Wah, W.W. Yu, Y.P. Liu, M.L. Mejia, J.C. Falkner, W. Nolte, V.L. Colvin, Photodegradation of Congo red catalyzed by nanosized TiO₂, *J. Mol. Catal. A* 242 (2005) 48–56.
- [6] N. Daneshwar, A. Oladegarazope, N. Djafarzadeh, Decolorization of basic dye solutions by Electrocoagulation: an investigation of the effect of operational parameters, *J. Hazard. Mater.* B129 (2006) 116–122.
- [7] A.F. Alshamsi, A.S. Albadwawi, M.M. Alnuaimi, M.A. Rauf, S.S. Ashraf, Comparative efficiencies of the degradation of crystal violet using UV/hydrogen peroxide and Fenton's reagent, *Dyes Pigm.* 74 (2007) 283–287.
- [8] (a) M.K. Purkait, S.S. Vijay, S. DasGupta, S. De, Separation of Congo red by surfactant mediated cloud point extraction, *Dyes Pigm.* 63 (2) (2004) 151–159; (b) M.K. Purkait, S. DasGupta, S. De, Resistance in series model for micellar enhanced ultrafiltration of eosin dye, *J. Colloid Interface Sci.* 270 (2004) 496–506.
- [9] Z.U. Rehman, I.H. Farooqi, S. Ayub, Performance of biofilter for the removal of hydrogen sulphide odour, *Int. J. Environ. Res.* 3 (4) (2009) 537–544.
- [10] P. Canizares, F. Martinez, M.A. Rodrigo, C. Jiménez, C. Saez, J. Lobato, Modelling of wastewater electrocoagulation processes Part II: Application to dye-polluted wastewaters and oil-in-water emulsions, *Sep. Purif. Technol.* 60 (2) (2008) 147–154.
- [11] N. Maximova, O. Dahl, Environmental implications of aggregation phenomena: current understanding, *Curr. Opin. Colloid Interface Sci.* 11 (4) (2006) 246–266.
- [12] M. Kobya, H. Hiz, E. Senturk, C. Aydinler, E. Demirbas, Treatment of potato chips manufacturing wastewater by electrocoagulation, *Desalination* 190 (2006) 201–211.
- [13] E.A. Viik, D.A. Carlson, A.S. Eikum, T. Gjessing, Electrocoagulation of potable water, *Water Res.* 18 (1984) 1355–1360.
- [14] P.R. Kumar, S. Chaudhari, K.C. Khilar, S.P. Mahajan, Removal of arsenic from water by Electrocoagulation, *Chemosphere* 55 (2004) 1245–1252.
- [15] K.V. Drondina, I.V. Drake, Electrochemical technology for fluorine removal from underground and waste waters, *J. Hazard. Mater.* 37 (1994) 91–100.
- [16] M. Kobya, E. Demirbas, O.T. Can, M. Bayramoglu, Treatment of levafix orange textile dye solution by electrocoagulation, *J. Hazard. Mater.* 132 (2006) 183–186.
- [17] Y. Yavruz, EC and EF processes for the treatment of alcohol distillery wastewater, *Sep. Purif. Technol.* 53 (1) (2007) 135–140.
- [18] H. Zhian, K. Khalipour, H. Khandani, The removal acid red 88 from aqueous solution by electrocoagulation, *World Appl. Sci. J.* 13 (3) (2011) 558–563.
- [19] M. Carmona, M. Khemis, J.P. Leclerc, F. Lapique, A simple model to predict the removal of oil suspensions from water using electrocoagulation technique, *Chem. Eng. Sci.* 61 (2006) 1233–1242.
- [20] F. Lapique, M. Carmona, M. Khemis, J.P. Leclerc, G. Tanguy, G. Valentin, Treatment of industrial liquid wastes by electrocoagulation: experimental investigations and an overall interpretation model, *Chem. Eng. Sci.* 61 (2006) 3602–3609.
- [21] Ching-Yao Hu, Shang-Lien Lo, Wen-Hui Kuan, Simulation the kinetics of fluoride removal by electrocoagulation (EC) process using aluminum electrodes, *J. Hazard. Mater.* 145 (2007) 180–185.
- [22] J.P. Kushwaha, V.C. Srivastava, I.D. Mall, Studies on electrochemical treatment of dairy wastewater using aluminum electrode, *AIChE J.* 57 (9) (2011) 2589–2598.
- [23] J. Del Nero, A. Galembeck, S.B. Costa-Silva, J.A. Pereira da Silva, Dye incorporation in polyphosphates gels: synthesis and theoretical calculations, *Mater. Res.* 6 (3) (2003) (São Carlos: On-line ISSN 1980-5373).
- [24] H. Zollinger, *Color Chemistry: Syntheses, Properties and Applications of Organic Dyes and Pigments*, CVH Publishers, Weinheim (Ge), 1987.
- [25] S.F. Beach, J.D. Hepworth, D. Mason, E.A. Swarbrick, A kinetic study of the hydrolysis of crystal violet and some terminal and bridged analogues, *Dyes Pigm.* 42 (1999) 71–77.
- [26] A. Ouerdia, Amélioration de la technique de défluorisation par le nouveau procédé d'électrocoagulation bipolaire, PhD/Thèse de la Faculté des sciences de l'université Mouloud Mammeri de Tizi Ouzou, Algeria, 2011.
- [27] M.Y.A. Mollah, P. Morkovskiy, J.A.G. Gomes, M. Kesmez, J. Parga, D.L. Cocke, Fundamentals, present and future perspectives of electrocoagulation, *J. Hazard. Mater.* 114 (1–3) (2004) 199–210.

- [28] G. Chen, P.L. Yue, Electrocoagulation and electroflotation of restaurant wastewater, *J. Environ. Eng.* 126 (9) (2000) 858–863.
- [29] W. Stumm, J.J. Morgan, *Aquatic Chemistry-Chemical Equilibria and Rates in Natural Waters*, third ed., John Wiley, New York, 1995.
- [30] J. Duan, J. Gregory, The influence of silicic acid on aluminum hydroxide precipitation and flocculation by aluminum salts, *J. Inorg. Biochem.* 69 (1998) 193–201.
- [31] A. Gürses, M. Yalçın, C. Doğar, Electrocoagulation of some reactive dyes: a statistical investigation of some electrochemical variables, *Waste Manage.* 22 (5) (2002) 491–499.
- [32] N. Mameri, A.R. Yeddou, H. Lounici, D. Belhocine, H. Grib, B. Bariou, Defluoridation of septentrional Sahara water of North Africa by electrocoagulation process using bipolar aluminium electrodes, *Water Res.* 32 (1998) 1604–1612.
- [33] P.T. Spicer, S.E. Pratsinis, Coagulation and fragmentation: universal steady-state particle-size distribution, *AIChE J.* 42 (6) (1996) 1612–1620.
- [34] P.T. Spicer, S.E. Pratsinis, M.D. Trennepohl, G.H.M. Meesters, Coagulation and fragmentation: the variation of shear rate and the time lag for attainment of steady state, *Ind. Eng. Chem. Res.* 35 (1996) 3074–3080.
- [35] P. Canizares, M. Carmona, J. Lobato, F. Martínez, M.A. Rodrigo, Electrodisolution of aluminum electrodes in electrocoagulation processes, *Ind. Eng. Chem. Res.* 44 (12) (2005) 4178–4185.
- [36] J.F. Le Page, *Catalyse de contact Conception, préparation, et mise en œuvre des catalyseurs industriels*, Technip, Paris, 1978 (ISBN 2-7108-0329-1).